Journal of Hydroscience and Hydraulic Engineering
Vol. 29, No.1 May, 2011, 47-56

NUMERICAL SIMULATION ON ADVECTION DISPERSION PROCESSES IN A MOUNTAINSIDE SLOPE

By

Masahiko Saito

Organization of Advanced Science and Technology, Kobe University, Rokkodai-cho Nada, Kobe, Japan

Takumi Ishihara

Central Japan Railway Company, Nishinakajima Yodogawa, Osaka, Japan

and

Kei Nakagawa

Department of Environmental Sciences and Technology, Kagoshima University, Korimoto, Kagosima, Japan

SYNOPSIS

Illegal waste disposal on mountainsides is a serious problem in Japan. However, conventional approaches to the groundwater pollution problems focus mainly on urban areas or flat land. In this study, 3D numerical simulations of the advection dispersion phenomena in a simple slope under cyclic rainfall were carried out to investigate the effects of hydraulic conductivity or geometric relation between the source area and pumping well. The results of our investigation show that the slight change in the streamline or presence of seepage in the middle of the slope affects sensitively the observed concentration data at the observation well. The results obtained seem are useful for evaluating the contamination process in real slopes.

INTRODUCTION

The illegal disposal of industrial, medical, general, and other waste materials continues to be a serious problem in Japan. Strengthened regulatory controls and monitoring have arrested the rise in large-scale illegal disposal of industrial waste, but violations of general waste disposal regulations are still increasing in many regions.

Illegal disposal frequently occurs in mountain forests and riverbeds, where monitoring is difficult, and its adverse effects on the ecosystem and agricultural products are of particular concern, as harmful substances contained in wastes dumped on mountainsides tend to contaminate both soil and groundwater in river head regions. In some mountain districts where there is a lack of municipal water systems, it may in the worst case lead directly to health degradation if contaminated drinking water is consumed.

In Japan and other countries, research on soil and groundwater contamination and on rainfall infiltration of slopes has been highly active. Many investigations have been conducted on contaminant elution and chemical properties, chiefly on the basis of indoor experiments, which have revealed important findings(1),(2). In relation to the

transport processes, many types of mathematical models (e.g., advection-dispersion and multiphase flow analysis) have been proposed, and numerical simulations have been performed for various materials/substances(3),(4). Regarding slope infiltration, many experimental and analytical investigations have been carried out, chiefly from the perspective of landslide disaster prevention(5), (6).

Studies on groundwater contamination, however, have generally centered on elucidation and prevention of water contamination in cities and lowland regions, and very few investigations have been conducted on the effects of illegal dumping on mountainsides and other slopes. There are many unknown factors that influence the behavior of contaminants after their release in mountainous areas, such as the diluting effects of rainfall, the complex geometry of the rock bed, or rapid changes in groundwater levels. Cumulative knowledge from field measurements and analyses is also sparse and insufficient for systematic explication. As the saying goes, "Nothing is clear without on-site measurements".

In the present study, we focused on the assessment of the diffusion and dispersion behavior of water-soluble materials on three-dimensional slopes (low-solubility materials were not included in the investigation) based on a relatively simple model slope with cyclical rainfall, using numerical simulation relating to slope permeability, the influence of the relative location of contaminant source and well positions on contaminant transport, and other factors.

GOVERNING EQUATION

Saturated-unsaturated seepage analysis

The following equation is used as the governing equation(7),(8),(9):

$$(B+\beta S_s)\frac{\partial \psi}{\partial t}=\nabla\cdot\left[\mathbf{K}\cdot(\nabla\psi+\nabla Z)\right] \tag{1}$$

where B is the specific water capacity (= $\phi \mathrm{d}S_w/\mathrm{d}\psi$, where ϕ is porosity and S_w is saturation), S_s is specific storage coefficient, $\mathbf{K}$ is the hydraulic conductivity tensor, ψ is the pressure head, and Z is the elevation head. In the saturated zone ($S_w = 1$), $\beta = 1$, and in the unsaturated zone, ($S_w \neq 1$), $\beta = 0$. Also, $\mathbf{K}$ can be expressed as follows in terms of the relative permeability k_r and the saturated hydraulic conductivity **Ks**:

$$\mathbf{K} = k_r \cdot \mathbf{Ks} \tag{2}$$

The condition on boundary Γ_1, where the pressure is defined, is given by

$$\psi = \psi_1 \quad \text{on} \quad \Gamma_1 \tag{3}$$

On boundary Γ_2, where flux q is defined,

$$q = q_2 = -\mathbf{n}\cdot\mathbf{K}\cdot(\nabla\psi+\nabla Z) \quad on \quad \Gamma_2 \tag{4}$$

where $\mathbf{n}$ is the outwardly directed unit normal vector.

Soil Water Retention Curve

The relative permeability k_r is an essential parameter in the analysis of seepage. It is considered a function of saturation, and the saturation S_w is considered a function of capillary pressure ψ_c ($\equiv -\psi$). Of the many mathematical

models proposed to describe these relationships (water retention curve), the van Genuchten equation (10) is adopted in the present study:

$$S_e = \frac{S_w - S_r}{1 - S_r} = \left\{1 + (a\psi_c)^n\right\}^{-m} \tag{5}$$

where S_e is the effective saturation, S_r is the residual saturation, and α, n and m are parameters, where n and m are dimensionless and a has dimensions of the reciprocal of the pressure head. The parameters n and m are not independent, and they are related by

$$m = 1 - 1/n \tag{6}$$

The relative permeability and effective saturation are related as follows(11).

$$k_r = S_e^{\varepsilon}\left\{1 - \left(1 - S_e^{1/m}\right)^m\right\}^2 \tag{7}$$

where ε is a parameter related to the degree of interconnection among voids. Generally, a value of 0.5 is used for ε. Differentiation of Eq. (5) with respect to ψ_c and by rearranging the result gives

$$-\phi\frac{dS_w}{d\psi_c} = \phi amn(1 - S_r)(a\psi_c)^{n-1}\left\{1 + (a\psi_c)^n\right\}^{-m-1} \tag{8}$$

Thus, the water retention curve and relative permeability can be calculated if the parameters a, n and the residual saturation S_r are determined.

Advection-dispersion equation

The transport of soluble materials by groundwater flow can be expressed by the following governing equation (the advection-dispersion equation).

$$\theta\frac{\partial C}{\partial t} = \nabla\cdot(\theta\mathbf{D}\cdot\nabla C) - \mathbf{q}\cdot\nabla C \tag{9}$$

where C is the concentration, θ is the volumetric water content ($=\phi S_w$), $\mathbf{D}$ is the dispersion coefficient tensor, and $\mathbf{q}$ is the Darcy velocity vector. The component $\mathbf{D}$ of Eq. (9) may be expressed as(12)

$$\theta D_{ij} = \alpha_T|\mathbf{q}|\delta_{ij} + (\alpha_L - \alpha_T)\frac{q_i\cdot q_j}{|\mathbf{q}|} + D_m\theta\delta_{ij} \tag{10}$$

where α_L is the longitudinal dispersivity, α_T is the transverse dispersivity, q_i is the component of the Darcy velocity vector $\mathbf{q}$ in the direction i, D_m is the molecular diffusion coefficient, and δ_{ij} is the Kronecker delta vector component.

The boundary condition is defined in terms of concentration as

$$C = C_A \quad \text{on} \quad \Gamma_A \tag{11}$$

In terms of the concentration gradient it is

$$F = F_B = -\mathbf{n}\cdot(\theta\mathbf{D}\cdot\nabla C) \quad \text{on } \Gamma_B \tag{12}$$

In terms of flux it is

$$F = F_C = \mathbf{n}\cdot\left(\mathbf{q}C - \theta\mathbf{D}\cdot\nabla C\right) \quad \text{on } \Gamma_C \tag{13}$$

It is well known that discretization of Eq. (9) by the standard Galerkin method results in unstable solutions if the advective term is dominant. In the present study, explicit characteristic Galerkin method is used to reduce this instability(13).

SIMULATION MODEL

Flow domain

Figure 1 shows the basic concept of the model slope and the finite element mesh. In the present study, we investigated the patterns resulting from two different locations of the contaminant source. In Case-A, as shown in Figure 2(a), the source was 2m × 2m in size and was situated in a small valley near x=60 m, y=200 m, with analysis performed for just one-half of the domain because of the symmetry about the y-axis. In Case-B, as shown in Figure 2(b), the same contaminant source was situated near x=25 m, y=200 m.

In each case, a pumping well 1-m-square in the cross-section and 4 m in depth was located at x=60 m, y=40 m, and the change over time in the contaminant concentration in seepage water from this area was investigated.

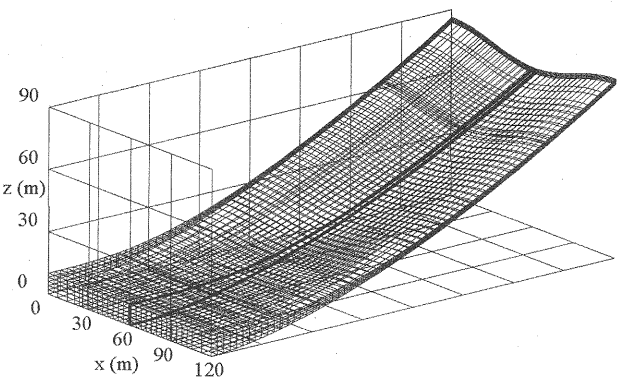

Fig. 1. Model slope concept

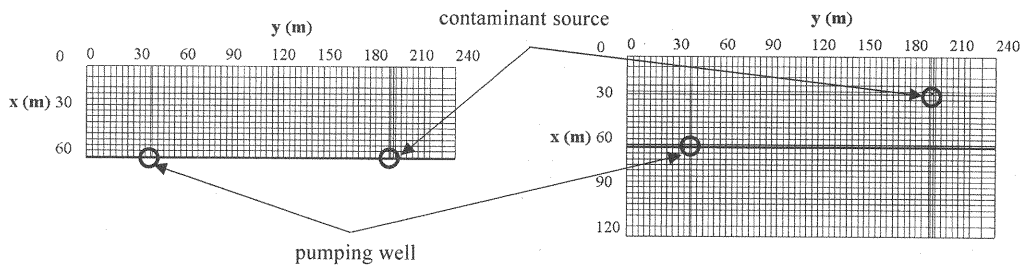

(a) Case-A (b) Case-B

Fig. 2. Location of contaminant source and pumping well.

Initial, boundary, and rainfall conditions

Figure 3 shows the initial unsaturated zone, saturated zone, and pressure head distribution. As shown in the figure, the height of the saturated zone was initially set at 8.1 m from the bottom surface at the downstream border, with the unsaturated zone lying above the saturated zone. The pressure distribution was initially hydrostatic up to a level of +2 m from the groundwater surface, and a constant value of –2 m above that level. The initial concentration distribution was set at C=1 at the ground surface at the contaminant source, and C=0 in all other zones. The boundary condition for seepage was set at a hydrostatic pressure distribution at y=0 m, z<8.1 m, and the ground surface and the well interior were defined as the seepage surface boundary, $q = 0$ when $\psi < 0$, and $\psi = 0$ when $q < 0$. In the advection-dispersion equation, the concentration was set at C=1 on the ground surface at the contaminant source, and the concentration gradient was set at F_B=0 at all other points on the ground surface and the boundary at the downstream border.

The rainfall conditions chosen were a period of precipitation (200 mm in 2 days) throughout the ground area beginning every 30 days, with the time-based precipitation waveform shown in Figure 4.

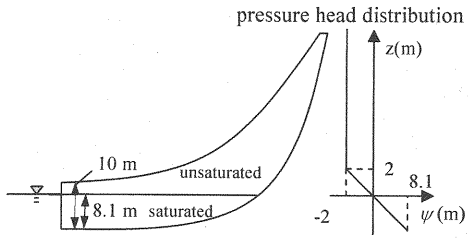

Fig. 3. Initial pressure head distribution.

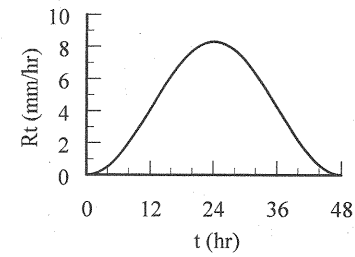

Fig. 4. Rainfall waveform.

Soil properties

Saturated hydraulic conductivity was assumed to be isotropic and homogeneous, and was given as K_s=1.0×10^{-4} (m/s) and as K_s=1.0×10^{-5} (m/s) for both Case-A and Case-B, resulting in a total of four cases. The porosity was taken as ϕ=0.4, and hysteresis was applied in relation to the water retention curve, by the method of Scott *et al.*(14). The main wetting and drying curves were distinguished by replacing α in Eq. (5) with α_w and α_d, respectively, with α_w=2α_d in accordance with Luckner *et al.*(15). Their values were as shown in Table 1.

The dispersivity used in Eq. (9) was regarded as a microscopic dispersion only, and taken as α_L=5.0×10^{-3}m, α_T =5.0×10^{-4}m, and the molecular diffusion coefficient was taken as D_m=1.0×10^{-9} m^2/s.

Table 1. Soil properties.

	K_s(m/s)	n	a_w(1/m)	a_d(1/m)	S_r
Case-A1 Case-B1	1.0×10^{-4}	3	3.4	1.7	0.10
Case-A2 Case-B2	1.0×10^{-5}	3	2.0	1.0	0.25

RESULTS AND DISCUSSION

Change in concentration at pumping well over time

Figure 5 shows the change in the contaminant concentration of the seepage from the pumping well for each case. The time of the arrival of contaminants at the well, after contaminant placement at the source location, was Day 50 in Case-A1 and Case-B1, and approximately Day 280 in Case-A2 and Case-B2. The peak concentration was found to vary within an overall range of 0.05%~0.25% of the concentration at the source. A trend reversal between the two contaminant source locations regarding the concentration rise following the arrival of contaminants at the well was observed. For the Case-A, the rise in concentration was larger for high permeability (Case-A1) than for low permeability (Case-A2), but for the Case-B the rise was larger for low permeability (Case-B2) than for high permeability (Case-B1). The reason for this is discussed in the section below.

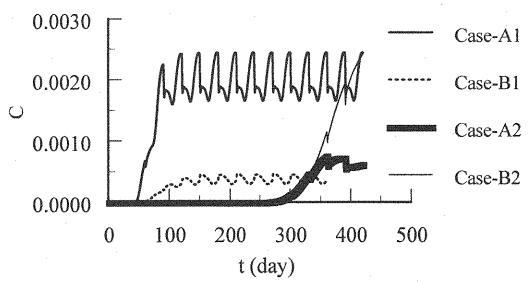

Fig. 5. Change in concentration over time.

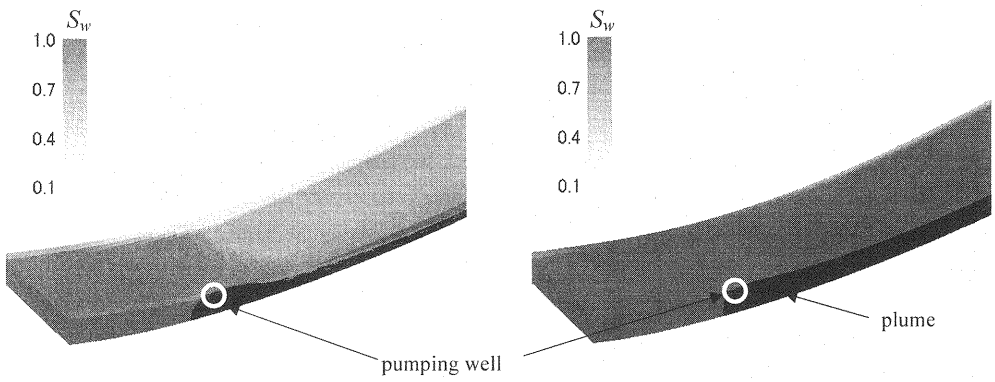

(a) Case-A1 (b) Case-A2

Fig. 6. Plume(C>0.001) and saturation distributions in well vicinity on Day 360 with Case-A contaminant source location.

Comparison of Case-A1 and Case-A2

Figure 6 shows the plume(C>0.001) and saturation distribution in the vicinity of the well on Day 360 for the Case-A location of the contaminant source. As indicated, in Case-A1 the saturation was generally small in the upstream region and the direction of seepage was downstream along the ground basement surface, but in Case-A2 the groundwater surface depth was near the ground surface. Figure 7 shows the saturation distribution at the ground surface in Case-A1 at the time of a peak rainfall and in Case-A2 just before the next rainfall (28 days after the previous rainfall).

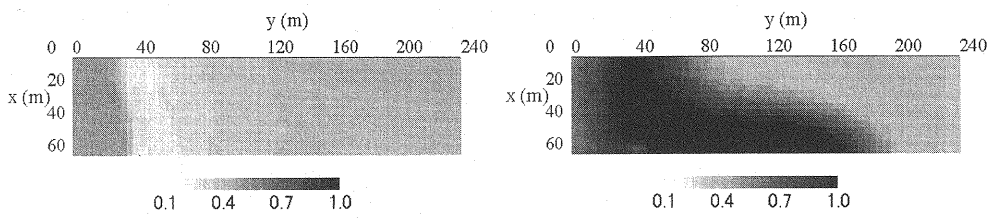

(a) Case-A1 (t=331 days; during peak rainfall) (b) Case-A2 (t=330 days; just before rainfall)

Fig. 7. Saturation distribution at ground surface.

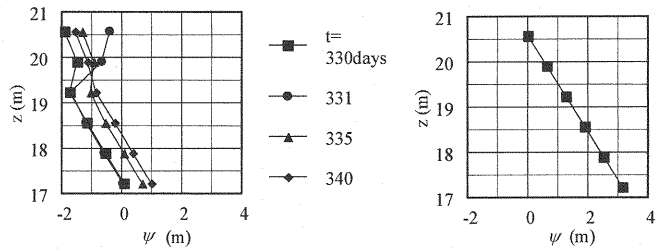

(a) Case-A1 (b) Case-A2

Fig. 8. Vertical pressure head distribution at x=60 m, y=102 m at t=330 days (just before rainfall) to t=340 days (8 days after rainfall).

In Case-A1, a generally unsaturated state was maintained throughout most of the region even during a period of rainfall, but in Case-A2 a broad zone of saturation or near-saturation persisted, centered in the valley depression, even 28 days after the previous rainfall.

This indicates that in the saturated zone in Case-A2 groundwater seepage from the ground surface occurs over a large region. Figure 8 shows the vertical pressure head distribution at x=60 m, y=102 m, at t=330 days (just before rainfall) to t=340 days (8 days after rainfall) in Case-A1 and Case-A2. In Case-A1, the pressure head distribution changes in response to the rainfall. In Case-A2 it shows no response, and at the ground surface the pressure head exhibits a hydrostatic pressure distribution equal to ambient atmospheric pressure, the sign of a seepage face, and the occurrence of contaminant discharge from the seepage face may therefore be inferred in this type of ground surface.

In short, the results suggest that in Case-A1, all of the contaminants that infiltrated from the contaminant source seeps from the pumping well, but in Case-A2, the contaminant discharge from the ground surface is subtracted from the infiltrating contaminant and the concentration in the well is thereby lowered. It should be noted, however, that the possibility of its recharge following discharge from the ground was not considered in the present study, and that diffusion of contaminants may actually be more rapid and cover a broader area than predicted from this simulation.

Comparison of Case-B1 and Case-B2

Figure 9 shows the plume(C>0.001) and saturation distributions in the vicinity of the well on Day 360 with the Case-B the contaminant source location. The saturation distributions are similar to those of Case-A1 and Case-A2, except that in Case-B1 the plume extends past the pumping well and on to the lower border of the valley region.

In Case-B2, in contrast, the plume does not extend downstream from the well. Figure 10 shows the streamlines originating in the vicinity of the contaminant source at t=380 days, which also indicates that the water catchment area is somewhat larger in Case-B2 than in Case-B1.

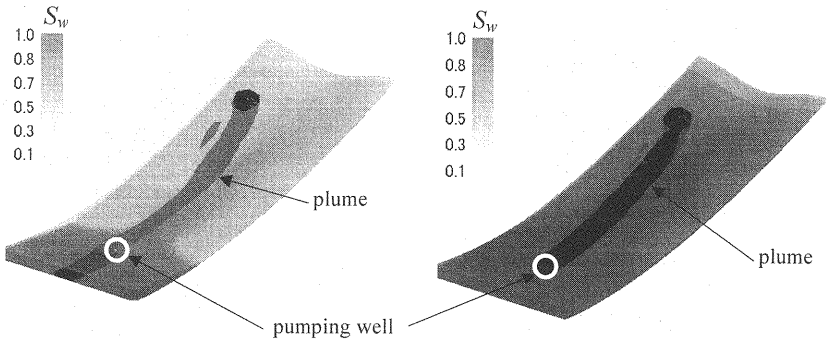

(a) Case-B1 (b) Case-B2

Fig. 9. Plume(C>0.001) and saturation distributions on Day 360 with Case-B contaminant source location.

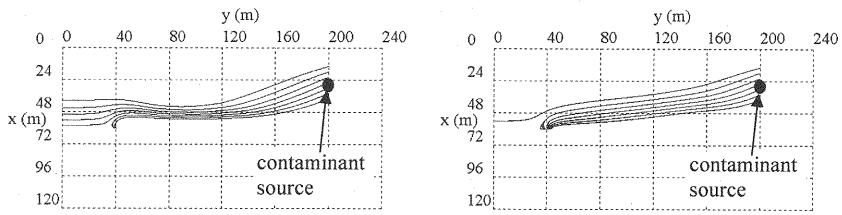

(a) Case-B1 (b) Case-B2

Fig. 10. Streamlines originating in vicinity of contaminant source at t=380 days.

A major difference between Case-A2 and Case-B2 is that in Case-B2 the flow does not proceed through valley regions with a large amount of seepage. This indicates that in Case-B2, the concentration in the pumping well becomes relatively high because effluence from the downstream border and the ground surface is relatively small.

These findings, taken together, indicate that the results of concentration measurements at pumping wells and monitoring respond in a highly sensitive manner to the presence and quantity of effluence in the upstream regions and to slight differences in streamlines, Therefore, it is important to determine as accurately as possible the flow field properties for accurate estimations and for predictions of contamination conditions by numerical modeling.

CONCLUSIONS

In the present study relating to diffusion and dispersion of water-soluble contaminating materials in a three-dimensional slope, we applied a numerical simulation using a relatively simple model slope to investigate the influence of the slope permeability, the relative locations of contaminant source and pumping well, and other elements affecting contaminant transport. The findings were as follows,

1) In cases where the saturated hydraulic conductivity was relatively low, discharge from the valley region may have occurred because of the groundwater level readily rises, thus suggesting that contaminants which have infiltrated the ground may re-emerge in the surface water flow.

2) Different saturated hydraulic conductivities lead to different water levels and pressure head distributions (and thus different streamlines), and the plume shape also changes accordingly, and may therefore result in different downstream arrivals.

3) Concentrations obtained by measurements at pumping and observation wells are highly sensitive to the presence of and quantity of effluence and slight changes in streamlines along the slope. In conjunction with such measurements it is important to determine the properties of the flow field.

In further studies, we plan to implement more realistic simulations by means of inclusion of basement non-uniformity, complex slope conditions, and other elements, with the ultimate goal of applying the simulation methodology to actual slopes.

Acknowledgements: We gratefully acknowledge the support of this study by a grant-in-aid from the Japan Society for the Promotion of Science (Grant-in-Aid for Scientific Research (C), Project Title: "Analysis of Contaminant Diffusion in Illegal Waste Dumping on Mountain Slopes", Project No. 21510031, Principal Investigator: Masahiko Saito).

REFERENCES

1. Hioki, K. and Aoki, K. : Basic research on adsorptive and desorptive characteristics of electrolytes from soil particles and formulation of equation, JSCE Journal of Geotechnical and Geoenvironmental Engineering, Vol.62 No.4, pp.840-857, 2006.
2. Nakagawa, K., Amamoto, A., Sekioka, Y. and Momii, K.: Laboratory experiment on reactive transport in physically and chemically heterogeneous field, Annual Journal of Hydraulic Engineering, JSCE, Vol.52, pp.397-402, 2008.
3. Nishigaki, M. and Kanno, Y.: Basic experimental research on oil contamination of subsurface material: JSCE Journal of Geotechnical and Geoenvironmental Engineering, Vol.63 No.1, pp.249-268, 2007.
4. Kobayashi, K., Hinkelmann, R., Helmig, R., Takara, K. and Tamai, N.: A Numerical experiment with two-phase and two -phase/three component models for the Methane migration in the subsurface aquifer, JSCE Journal of Hydraulic, Coastal and Environmental Engineering, Vol.63 No.2, pp.120-133, 2007.
5. Kitamura, R., Sako, K., Kato, S., Mizushima, T. and Imanishi, H..: Soil tank test on seepage and failure behaviors of Shirasu slope during rainfall, Japanese Geotechnical Journal, Vol.2,No.3 pp.149-168, 2007.
6. Awal, R., Nakagawa, H., Kawaike, K., Baba, Y. and Zhang, H.: Numerical and experimental study on 3d transient seepage and slope stability of landslide dam failure, Annual Journal of Hydraulic Engineering, JSCE,, Vol.52, pp.61-66, 2009.
7. Neuman, S. P.: Saturated unsaturated seepage by finite elements, Proc., ASCE HY, Vol.99, No.12, pp.2233-2250, 1973.
8. Neuman, S. P.: Galerkin method of analyzing non-steady flow in saturated-unsaturated porous media, Finite element Method in flow problem, edited by C. Taylor, O.C. Zienkiewicz, R.H. Gallagher, John Wiley & Sons, Chap.19, 1974.
9. Akai, K., Ohnishi, Y. and Nishigaki, M.: Finite element analysis of saturated-unsaturated seepage in soil, Proceedings of the Japan Society of Civil Engineering, No.264, pp.87-96, 1977.
10. van Genuchten, M. T.: A closed-form equation for predicting the hydraulic conductivity of unsaturated soils, Soil Science Society of America Journal, Vol.44, pp.892-898, 1980.
11. Maulem, Y. :A new model for predicting the hydraulic conductivity of unsaturated porous media, Water Resources Research, Vol.12, pp.513-522, 1976.
12. Bear, J. :Dynamics of Fluid in Porous Media, Elsevier, New York, 1972.
13. Zienkiewicz, O. C. and Taylor, R. L.: The Finite Element Method, Vol.3, (5th ed.), Butterworth-Heinemann,

pp.13-63, 2000.

14. Scott, P. S., Farquhar, G. J. and Kouwen, N. :Hysteretic effects on net infiltration, pp.163-170, In Advances in Infiltration, Am. Soc. Agric. Eng., St. Joseph, MI, 1983.
15. Luckner, L., van Genuchten, M.T. and Nielsen, D.R.: A consistent set of parametric models for the subsurface, Water Resources Research, Vol.25, pp.2187-2193, 1989.

APPENDIX – NOTATION

The following symbols are used in this paper:

a = VG parameter;
a_d = VG parameter(drying curve);
a_w = VG parameter(wetting curve);
B = specific water capacity;
C = concentration;
D_m = molecular diffusion coefficient;
$\mathbf{D}$ = dispersion coefficient tensor;
k_r = relative permeability;
K_s = saturated hydraulic conductivity;
$\mathbf{K}$ = hydraulic conductivity tensor;
$\mathbf{K}_s$ = saturated hydraulic conductivity tensor;
m = VG parameter;
n = VG parameter;
$\mathbf{n}$ = outwardly directed unit normal vector;
q_i = component of the Darcy velocity vector $\mathbf{q}$ in the direction i.
$\mathbf{q}$ = Darcy velocity vector;
S_e = effective saturation;
S_r = residual saturation;
S_s = specific storage coefficient;
S_w = degree of saturation;
t = time;
x, y, z = Cartesian coordinates;
Z = elevation head;
α_L = longitudinal dispersivity;
α_T = transverse dispersivity;
δ_{ij} = Kronecker delta vector component;
ε = parameter related to the degree of interconnection among voids.
ϕ = porosity;
θ = volumetric water content;
ψ = pressure head;
ψ_c = capillary pressure;

(Received Aug, 01, 2010 ; revised Mar, 07, 2011)